Chem Soc Rev

This article was published as part of the

2009 Green Fluorescent Protein issue

Reviewing the latest developments in the science of green fluorescent protein

Guest Editors Dr Sophie Jackson and Professor Jeremy Sanders

All authors contributed to this issue in honour of the 2008 Nobel Prize winners in Chemistry, Professors Osamu Shimomura, Martin Chalfie and Roger Y. Tsien

Please take a look at the issue 10 table of contents to access the other reviews

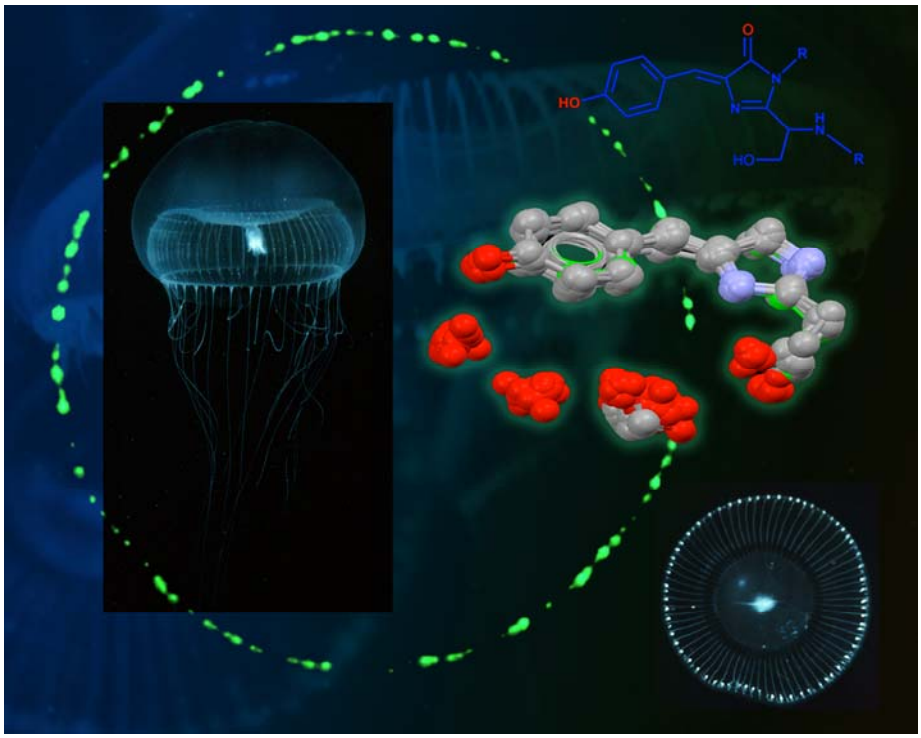

The photochemistry of fluorescent proteins: implications for their biological applications†

Harriet E. Seward and Clive R. Bagshaw*

Received 15th May 2009
First published as an Advance Article on the web 4th August 2009
DOI: 10.1039/b901355p

Green fluorescent protein from *Aequorea victoria*, its relatives and derivatives are ubiquitous in their use as biological probes. In this *tutorial review*, we discuss the photochemistry of this fascinating class of proteins and illustrate some of their advantages and drawbacks in a range of applications. In particular, we focus on the ionisation states of the chromophore and how they are affected by internal and external proton transfer. Light-induced reversible and irreversible events are discussed in terms of the underlying chromophore structure. These phenomena have an influence on the interpretation of FRET (Förster resonance energy transfer), FRAP (fluorescence recovery after photobleaching), as well as single molecule studies.

Introduction

Green fluorescent protein was originally extracted from the jellyfish *Aequorea victoria*, but many derivatives have been constructed using protein engineering to provide a wide range of probes for biological systems. While characterisation of the chemical and photophysical properties of GFP has helped to design some of these mutations in a rational manner, fine tuning has usually been achieved by random mutagenesis followed by selection of desired properties. The enhanced properties of these mutants, in turn, have provided insights into the complexities of autofluorescent proteins. In this review we start with some well-characterised properties of GFP and then comment on more recent constructs and some of their potential applications.

Department of Biochemistry, University of Leicester, Henry Wellcome Building, Lancaster Road, Leicester, UK LE1 9HN. E-mail: crb5@le.ac.uk; Fax: +44 (0)116 229 7018; Tel: +44 (0)116 229 7048

† Part of a themed issue on the topic of green fluorescent protein (GFP) in honour of the 2008 Nobel Prize winners in Chemistry, Professors Osamu Shimomura, Martin Chalfie and Roger Y. Tsien.

AvGFP

Wild-type green fluorescent protein (avGFP)[1] from the jellyfish *A. victoria* is a spectroscopically-fascinating protein in its own right and remains of great interest to physicists and chemists. Its fluorescent chromophore forms spontaneously in the presence of O_2 from residues 65–67 (Ser-Tyr-Gly) without the need for additional cofactors or coenzymes and was identified as *p*-hydroxybenzylideneimidazolinone.[2–4] Outside the robust β-barrel structure of avGFP, the chromophore is only weakly fluorescent at room temperature. Consequently it is concluded that the β-barrel restrains the rotational and vibrational dynamics of the excited state of the chromophore,

Harriet E. Seward

Harriet Seward received her PhD (thesis title 'Magneto-optical Spectroscopy of Hemoproteins') from the University of East Anglia in 1999. She undertook post-doctoral studies on multiheme cytochromes with Professors Andrew Thomson and David Richardson (1999–2003). In 2004, she moved to the University of Leicester to research spectroscopy and enzymology of P450 redox systems from Mycobacterium tuberculosis *with Professor Andrew Munro. Currently, she is studying the interesting photophysical behaviour of a variety of fluorescent proteins (FPs) with Professor Clive Bagshaw—funded by the Leverhulme Trust—and is particularly interested in protonation reactions of the yellow FPs.*

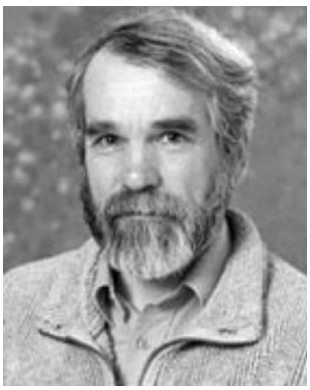

Clive R. Bagshaw

Clive Bagshaw has investigated the function of myosin for nearly 40 years using fluorescence and kinetic assays. It was during the characterisation of a GFP–myosin fusion protein intended for Förster resonance energy transfer (FRET) measurements that he became interested in the complexities of GFP. Since then, he has applied kinetic methods at the ensemble and single molecule level to study the photochemistry and protonation of GFP variants.

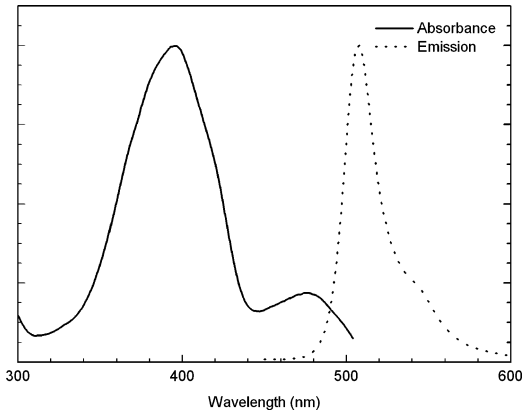

Fig. 1 Wild-type avGFP absorbance (solid line) and emission (dotted line) spectra. Data courtesy of Dr Jasper Van Thor, Imperial College London.

which would otherwise lose energy *via* a radiationless pathway. The absorption spectrum of avGFP contains two peaks at 395 and 475 nm which both emit light at ~510 nm when excited (Fig. 1). These peaks were identified as the neutral (phenolic) and anionic (phenolate) forms of the chromophore.[5] In wtGFP, the majority ground-state species (~80%) is stabilised in the neutral form by a hydrogen-bonding network which includes water molecules, and the residues Ser205 and Glu222.

Under UV illumination, the proportion of the anionic form is increased with a shifted absorbance at 483 nm. This was shown to result from the decarboxylation of Glu222.[6] The decarboxylated form is similar to the stabilised anionic forms of GFP mutants such as Glu222Gln and Ser65Thr, in which the hydrogen-bonding network is also disrupted. This decarboxylation and subsequent increase in fluorescence brightness is an example of an irreversibly photoactivated protein.

A reversible photoactivation of the GFP chromophore occurs in an anaerobic environment. At low oxygen concentrations, the anionic peak of the avGFP chromophore can be excited by a 488 nm laser to become a red-emitting form with a broad emission that peaks at 590 and 600 nm and an additional excitation peak at 525 nm.[7]

Initial studies of wild-type GFP indicated that, in addition to the neutral and anionic forms of the chromophore (denoted A and B for acid and basic forms, respectively), there was at least one other ground state, denoted I, an intermediate deprotonated form that possibly has the hydrogen-bonding scaffold of the neutral chromophore.[8] The emission at 510 nm characteristic of the anionic state, even when the protonated state is excited, indicates very rapid loss of the proton (*i.e.* excited-state proton transfer, ESPT). The excited state of the phenol group is more acidic than its ground state.[9] Potential proton acceptors are likely to come from the hydrogen-bonding network that surrounds Tyr66 of the chromophore and include the side chains of His148 and undecarboxlated Glu222 (Fig. 2). This is an internal proton transfer.

The chromophore is shielded from the bulk pH of the solution, but there is a suggested 'proton wire' of water molecules and internal residues that could run from Glu222

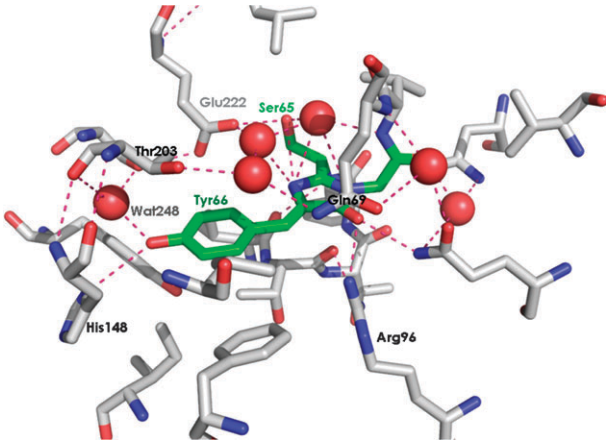

Fig. 2 Chromophore pocket of avGFP adapted from Protein Databank Structure using Pymol.[10] Chromophore shown in green, water molecules in red, hydrogen bonds by dashed pink lines.

to Glu5 at the bottom of the β-barrel.[11–13] Rotation of Thr203 could also move a proton onto the backbone carbonyl of His148 and from there, out into the bulk solvent.[14]

The observed macroscopic pK values obtained by titration can be interpreted in terms of microscopic pK values together with the equilibria for internal proton exchange (see Fig. 3). Titration of avGFP yields two pK values, $pK_1 \approx 5$ and $pK_2 \approx 11.5$. In terms of equilibrium dissociation constants, the macroscopic constant $K_1 = K_{AA} + K_{BB}$, while $1/K_2 = 1/K'_{AB} + 1/K_{BB}$. To maintain thermodynamic balance, $K_{AB}/K_{AA} = K'_{AB}/K_{BB} = K_{IP}$, where the latter is the equilibrium constant for internal proton transfer and ~0.25 for avGFP. From this information it can be determined that the microscopic pK values are $pK_{AA} = 5.1$, $pK_{AB} = 5.7$, $pK_{BB} = 11$ and $pK'_{AB} = 11.6$. Thus at pH 7 the dominant state is the protonated chromophore with a deprotonated internal ligand (ChroH. R^-; 80%, see Fig. 3) which is in equilibrium with the deprotonated chromophore with a protonated internal ligand ($Chro^-$. RH; 20%) *via* internal proton transfer, while the other states associated with protein exchange with the solvent are of minor consequence. With GFP mutants, however, this is not always the case.

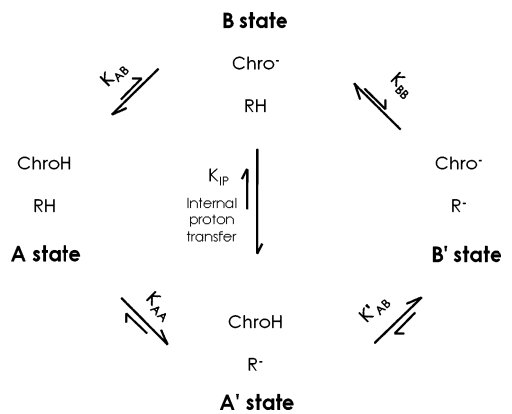

Fig. 3 Ground state equilibria of chromophore (Chro) and internal ligand (R). Titrations of pH follow the overall transition of A to B states. The double deprotonated B-state is achieved only at very high pH, in avGFPs where Glu222 is the titratable residue.

AvGFP is a dimer in solution as well as in crystal form with a K_d of approximately 100 μM. Early studies on wild-type GFP showed that self-association at high protein concentrations gave a spectral change (peak *ca.* 395 nm) similar to that produced by protonation.[3]

Mutants of avGFP

AvGFP has been subjected to a variety of improvements, for its application as a biological probe, *e.g.* to improve brightness and folding efficiency at 37 °C, change absorption and emission wavelengths, decrease chromophore maturation times and sensitivities to pH and simple anions and to favour monomers.

Brightness can be improved by stabilising the phenolate anion as mentioned previously, for example, with mutations at Ser65Thr, Ser205 and Glu222. A commonly used GFP is eGFP ('enhanced GFP'; Phe64Leu, Ser65Thr) which has a stabilised anionic chromophore (Ser65Thr) and enhanced folding (Phe64Leu).[3,15] The measured macroscopic pK_1 of 5.7 obtained from a pH titration of eGFP (Fig. 4) appears to be a simple deprotonation of the tyrosine ring within the chromophore (*i.e.* $\sim$pK_{AB} in Fig. 3) as a consequence of the internal proton transfer that strongly favours the $Chro^-$. RH state ($K_{IP} \approx 20$).

Well-known mutations that shift the emission wavelengths include changing the nature of the aromatic ring within the chromophore to a tryptophan (cyan FP) or histidine (blue FP). Mutations of Thr203 to an aromatic residue give rise to the yellow FP class of mutants as a result of π-stacking with the phenolate of the chromophore.[3] Extended π-systems can respond essentially instantaneously to a change in chromophore polarity by a shift of the π-electron cloud, preferentially stabilising the electronic state with the larger dipole moment, and leading to the shift to longer wavelength emission. The fluorescence of YFPs is, however, more sensitive to quenching by protonation, anion binding and photobleaching.

Protonation reactions and proton-coupled anion binding. When the pH of a YFP solution is rapidly changed, the fluorescence emission intensity responds on the seconds timescale. Protonation reactions are intrinsically rapid

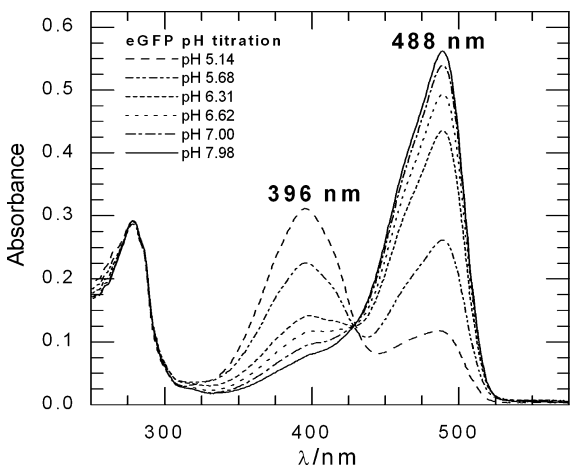

Fig. 4 pH titration of the eGFP variant. Data provided by Iman Alajeyan (MSc thesis, University of Leicester).

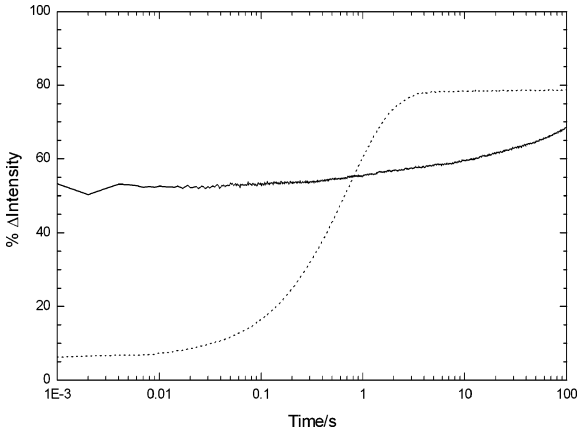

Fig. 5 YFP 10C A206K pH jump (100 mM KPi pH 5.4 *vs.* 200 mM KPi pH 8.1; endpoint pH 7.2) in the absence (solid line) and presence (dotted line) of 50 mM NaCl. Intensity given as a % of total change of signal (1, 1.7 V, respectively). 100% represents total signal at pH 8.1, 0% signal at pH 6.1. Endpoint = pH 7.1 [H. E. Seward, unpublished results].

(sub-ms timescales) and it is now known that the slow response is largely due to a coupled reaction with chloride present in the buffer. In the absence of chloride or other halides, when the pH is jumped, most of the reaction occurs within the dead time of the stopped-flow instrument but a residual slow reaction is still resolved on the seconds timescale (see Fig. 5), possibly due to a slow protein conformational rearrangement or binding of other anions in the buffer.

It has been shown that eYFP (also known as YFP 10C; Ser65Gly, Val68Leu, Ser72Ala, Thr203Tyr) is sensitive to simple anions, such as halides, nitrates and thiosulfate.[16] These bind to eYFP in positions near the chromophore (near Gln69) and raise the pK of the chromophore by inhibiting the development of its anionic form. Halide binding also shifts the absorption peak of the protonated A form of YFP from 420 to 395 nm. Other YFP-type mutants such as E^2GFP (eGFP Thr203Tyr) have a halide binding site in a different position that are directly above the imidazolone ring chromophore with hydrogen bonds to Tyr203, the backbone nitrogen of Gly67 and a water molecule (Fig. 6).[17,18] Of course, sensitivity to halide and pH can be turned to advantage as a biological sensor of chloride or intracellular pH. However, even eYFP Gln69Met (Citrine),[19] which was engineered to be less sensitive to chloride through steric hindrance at its binding site, retains some sensitivity to chloride, as discussed below. This reduced sensitivity lowers its pK and the mutation also renders the protein more photostable. Interestingly, binding of the thiocyanate anion to eYFP disrupts normal excited-state processes and allows direct emission at 475 nm from the neutral form of the chromophore.[20] This does not occur on halide binding. In the case of E^2GFP, significant emission at both 470 and 507 nm is observed in the mutant at pH 7 on excitation at 405 nm. Halide and thiocyanate binding suppress 507 nm emission. [H. E. Seward, unpublished results].

The sensitivity of eYFP to halides and other anions is well known[16] and therefore, less chloride sensitive variants such as superYFP, Citrine and Venus have been developed. They are indeed less sensitive and their higher K_d values may be

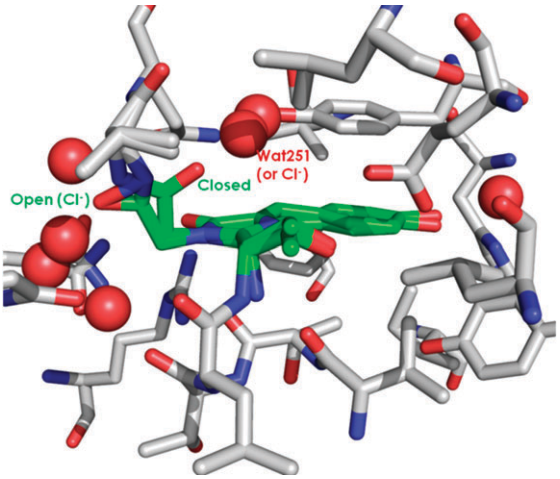

Fig. 6 'Open' and 'closed' forms of E^2GFP. Adapted using Pymol[10] from the structure 2H9W.[21] Waters 251 and 254 (red spheres) are found in slightly different positions for both forms. Water 257 is present only in the closed form. Chloride occupies the position occupied by Water 251 in the open conformation.

sufficient to avoid chloride-induced artifacts within living cells. However, in protein folding studies *in vitro* that use molar quantities of guanidine hydrochloride as a denaturant, it is likely that chloride binding will contribute to the fluorescent signal change and hence appropriate control measurements are required.

Dimerisation of avGFP variants. Dimerisation of eGFP increases the ratio of 390 to 488 nm absorbance in a similar manner to that of wild-type avGFP, and the increased absorbance at the protonated peak is retained at basic pH. However, this peak is not observed in the absorption spectrum of concentrated eYFP.[22] This was a surprising result given that sedimentation equilibrium analysis shows that both proteins dimerise with K_d values in the region of 100 μM. Also, eYFP has a higher pK than eGFP and hence is more susceptible to protonation by external solvent. Protonation of fluorescent proteins is a complex reaction and often involves, in addition to a fast phase (sub-ms), a slow (millisecond to second timescale) isomerisation of the protein and/or chromophore.[23] Association of these proteins at high concentrations presumably effects the conformation of the protein which, for GFP at least, affects the apparent pK of the chromophore. This reflects predominantly an internal proton rearrangement rather than a change in the external pK_a. In eYFP the greater accessibility of the chromophore to bulk pH must negate this internal proton shift.

Dimerisation of avGFP variants can be disrupted with a single Ala206Lys mutation in the centre of a large hydrophobic patch that is part of the dimer–dimer interface in crystal structures of avGFP variants.[24] In NMR studies this interface region has not been fully assigned presumably due to exchange broadening. Even with the mutant eYFP Ala206Lys, we have not assigned part of the backbone β10 helix that crystal structures indicate is involved in dimerisation, including the backbone carbonyls of Lys206. This suggests that monomer–dimer interactions, even with the Ala206Lys mutation, can occur in solution at an unfavourable exchange rate for detection with NMR. This residue was also unassigned in GFPuv (Phe99Ser, Met153Thr, Val163Ala).[25] There are also indications from NMR studies that Venus, an eYFP variant without the Ala206Lys mutation, can form both dimers and transient higher order oligomers in solution.[26]

ESPT in eYFPs? The internal proton equilibria in eYFP 10C favour the anionic state, and the protonated state is only occupied at low external pH (p$K \approx 6$, dependent on associated anions). Excitation of the protonated eYFP results in weak emission at 530 nm, indicative of a small contribution from ESPT. At high protein concentrations (100 μM), used for picosecond spectroscopy, a significant emission at 530 nm was observed, but this emission was accompanied by a change in the anisotropy.[23] Subsequent experiments demonstrated that under these conditions, the eYFP was forming 'hetero' dimers of protonated YFPH and anionic YFP^- with their dipoles oriented at around 65°.[20] Förster resonance energy transfer (FRET) from YFPH to YFP^- resulted in strong emission at 530 nm and a negative anisotropy, following excitation of YFPH at 390 nm. At low concentrations or with the Ala206Lys mutation, YFPH does emit very weak emission at 530 nm due to limited ESPT, but the YFPH excited state decays mainly by a radiationless pathway.

Fluorescent proteins from other sources

Variants of avGFP have produced a range of wavelength emissions from 400 to 530 nm. However, a protein with red wavelength emission would have a number of advantages for probing live cells and tissues: their lowered background fluorescence and scattering; decreased cell damage and greater depth of imaging from longer wavelength irradiation; their potential in dual colour applications and as novel FRET probes. AvGFP can emit red light under certain conditions, as mentioned earlier, and recently a mutant with some red emission has been obtained.[27] A tetrameric red-emitting FP, the now commonly called DsRed,[28] was discovered from the coral *Discosoma*. Here the conjugated π-system of the chromophore is extended through the formation of an acylimine bond. This protein has led to a range of orange, red and even purple mutants in the monomeric fruit series (mFruit).[29,30] Many other FPs and chromoproteins (CPs, non-fluorescent coloured proteins) have been isolated from Anthozoa species (corals, sea anemones). A common problem with these novel FPs can be their oligomeric state. Many of the native proteins are tetrameric which can lead not only to poor localisation and/or impaired function of a fusion partner but also cytotoxicity in live cells.

Acylimine bond formation is thought to proceed *via* an 'immature' green chromophore intermediate and involves a protein peptide isomerisation. The mature chromophore is shown in Fig. 7.

Like the variants of avGFP, the colour of emission is dependent on the chromophore environment. DsRed can be irreversibly converted into a 'super-red' emitting form with longer wavelength emission but lower brightness through decarboxylation of a local glutamate, Glu215. The mFruit variant, mPlum, owes its 650 nm emission to a hydrogen bond

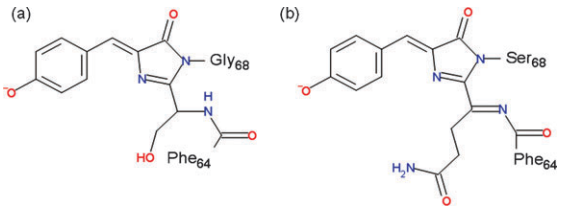

Fig. 7 Chemical structure of the GFP (a) and DsRed (b) chromophores showing the extended π-system of double bonds in the red chromophore.

between the carboxylate of another glutamate, Glu16 and the chromophore acylimine bond.[31,32] While the mFruit series have low external p*K* values (<5), at pH > 9.5, another pH dependent process is observed in the mStrawberry and mCherry variants, in which there is a blue shift in emission intensity that is associated with higher quantum yield.[33] Crystal structures indicate that the chromophore is more planar at higher pH and that Glu215 has changed conformation and is therefore likely to have become deprotonated.

A reversibly photoconvertible FP, Dronpa, developed from a FP found in the coral Pectiniidae,[34] switches reversibly between dark (protonated, A) and green (anionic, B) states on laser illumination at 405 (dark to green) and 490 nm (green to dark) on the seconds timescale. Dronpa has been described as having two protonated ground states, which do not readily interconvert under laser illumination at 405 nm (possibly ChroH RH and ChroH R^- previously illustrated in Fig. 3).[35] Dronpa has a waterfilled opening between β7 and β10 that connects the chromophore with bulk solvent. At low external pH it is probable that RH remains protonated in Dronpa. This property is similar to that of the aforementioned E^2GFP.[36]

The study of FPs and CPs has also led to a greater understanding of the nature of the light and dark states of the chromophore and an extended range of reversibly and irreversibly photoactivable FPs. This class of FPs are sometimes referred to as 'optical highlighter' proteins, that is, proteins whose fluorescent properties are changed with laser illumination.

Light and dark states in FPs and their structural basis

The term 'dark state' refers to a non-fluorescent state of the chromophore, that is, a state that does not absorb at the excitation wavelength or upon excitation does not lead to fluorescence emission. In the FP chromophore, light-induced dark states can be reversible or irreversible (photobleached). The former can lead to unusual behaviour in single molecule studies such as rapid on–off cycling also known as 'blinking' or 'flickering'. There is much interest in the nature of these reversible and irreversible dark states. Theories include protonation of the chromophore, *cis–trans* isomerisation of the protein chromophore (with or without accompanying protonation), or formation of zwitterionic or neutral dark forms that differ from the protonated form at low external pH.

The absorption spectrum of E^2GFP (Phe64Leu, Ser65Thr, Thr203Tyr), a FP in the yellow class, in phosphate buffered saline is dominated by neutral dark forms of the chromophore and contains bands from three distinct species, the aforementioned A and B states and a third neutral non-radiative state (C), absorbing at ~365 nm.[36] This was initially suggested to be a neutral chromophore with decreased hydrogen bonding with respect to the A form. Independent photoswitching between the anionic B and protonated C forms is observed using the appropriate lasers. Later structures of E^2GFP at pH 9.0 show the chromophore to exist in two conformations (described as 'open' and 'closed') in which the chromophore O3 peptide bond (from Gly67) flips (see Fig. 6).[21] Increase of the 'C' form is also observed concomitantly with an increase in chloride concentration at pH between 5 and 9. The chloride-bound structure[17] shows a conformational change which is equivalent to the open conformation observed in the E^2GFP crystal at pH 9.0 and that was attributed to the neutral A and anionic B states with a protonated internal residue (Glu222). This suggests that the easily convertible forms C and B are already in the open configuration.

A recent burst of crystallographic structures of photoactivable FPs has added weight to the theory that *cis–trans* isomerisation of the chromophore is the mechanism that is responsible for the existence of, or switching between, fluorescent and non-fluorescent (or dark) forms of FPs. This *cis–trans* isomerisation occurs around the C=C double bond between the ring structures (exocyclic) within the chromophore (Fig. 8) and is not related to the aforementioned peptide bond flip observed in E^2GFP. The *cis–trans* transition is often suggested to be driven or accompanied by protonation of the chromophore. Protonation would occur on a much faster timescale than isomerisation of the chromophore.

Structural determination of FPs and CPs indicates that non-planar *trans* forms of the chromophore are often associated with non-fluorescent chromoproteins, whereas most light-emitting states of FPs are found to crystallise with their chromophore in a planar *cis* conformation. However, there are exceptions: the chromophore of the fluorescent eqFP611 from *Entacmaea quadricolor* crystallises in a planar *trans* conformation;[37] the chromophores of fluorescent mTFP1 (teal FP), which is based on cFP484 from the coral *Clavularia*, and some of the mFruit series have a non-planar *cis* conformation.[33,38] Indeed, there is some evidence to suggest that an irradiated sample of eqFP611, which loses fluorescence, may undergo a *trans–cis* isomerisation.[39]

Interestingly, recent NMR studies on Dronpa suggest that the protonated *trans* form of the chromophore is linked with

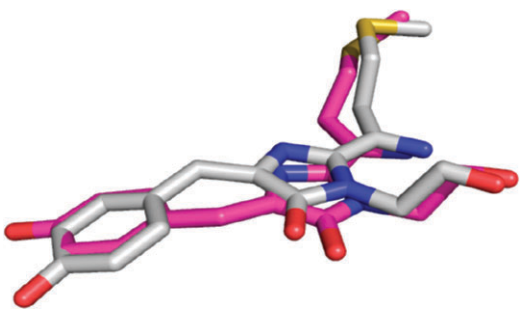

Fig. 8 *Cis* (magenta) and *trans* (grey) forms of asFP595 Ala143Ser figure adapted from Protein Databank structures 2A53 and 2A56[40] using Pymol.

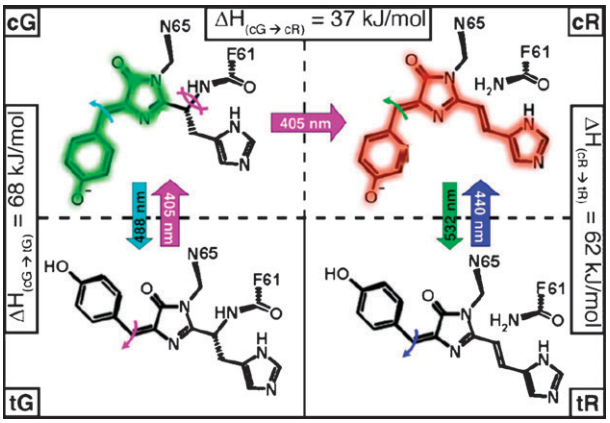

Fig. 9 Photoinduced transitions in IrisFP. Reproduced with permission from PNAS 2008. Structural motions induced by light are represented by curved arrows of the same colour used to represent light illumination at specific wavelengths. cG, *cis*-green; tG, *trans*-green; cR, *cis*-red; tR, *trans*-red. Enthalpies estimated from QM/MM molecular dynamics.

increased flexibility of the chromophore and the β-barrel and the flexibility rather than the conformation was suggested to be the source of its non-radiative excited state.[41]

It is not always stated explicitly in the literature whether the spectroscopy of the crystals has been shown to be consistent with the solution behaviour. However, a thorough study of a new 'optical highlighter' protein IrisFP, the F173S mutant of the tetrameric photoconvertible EosFP, links the spectroscopy to the behaviour in crystal and solution form.[42]

IrisFP can be reversibly converted between light and dark forms of a green FP, then irreversibly converted to a red form, which itself is reversibly switchable between red-emitting and dark forms. The light-induced irreversible step involves, along with the extension of the conjugated π-system, a peptide backbone cleavage shown in Fig. 9. The π-system of the chromophore is extended with respect to that of DsRed due to the presence the imidazole side chain in the chromophore amino acid triad.

In IrisFP, the *cis* forms of both the green and red forms are found to be light-emitting. The dark state of the green form has a non-planar *trans* chromophore. Its absorption spectrum shows increased absorbance at 390 nm so the chromophore is likely to be protonated. The crystal structure shows a hydrogen bond from the phenolic oxygen to a local water and Glu144, the latter ligand being likely to be deprotonated (ChroH R^-). Unfortunately the crystal form of the dark state of the red chromophore did not appear to be completely photoconverted and contained a mixture of *cis* and *trans* forms of the chromophore. This may have been due to poor penetration of the green light through the crystal. The presence of the *trans* conformer suggests that this form is a good candidate for the dark state of the red-emitting form. Interestingly, a recent study[43] of twelve orange and red-emitting FPs showed reversible red–green photoconversion in the variants mKate, its dimeric parent Katusha and the far-red emitter HcRed1 under excitation at 561 or 405 nm. The variants, mOrange1 and mOrange2 from the mFruits series showed orange to far-red conversion on excitation at 488 nm. Another mFruit, the commonly used red-emitter mCherry, did not exhibit any photoconversion. This study reinforces the necessity of using FPs with well-characterised photophysics in applications such as dual colour imaging and Förster resonance energy transfer and will be discussed further in the following section.

Implications of photophysics for applications

FPs have been developed as probes of biological systems by making fusion proteins with other proteins of interest.[44,45] This has proven a powerful approach, as the enormous literature attests. However, in order to interpret the fluorescence signals to yield valid information about the fusion protein, it is necessary to understand the complexities of the FPs themselves. Here, we consider a number of complications.

Single molecule studies

Single molecule measurements constitute a rapidly developing field with the advantage that they can overcome the ensemble averaging of traditional measurements and hence reveal hidden properties of a system. The high quantum yield and moderate photostability of many FPs has allowed their observation at the single molecule level using confocal and total internal reflection fluorescence (TIRF) microscopy. Single molecule studies generally require working concentrations of fluorophore of nanomolar or less, which are either immobilised or in solution. This ensures that the average separation distance between molecules exceeds the optical resolution limit of around 200 nm. The detection of single molecules requires maximising the detection efficiency while minimising the background signal. Usually high light intensities (such as generated by a focused laser beam) are required to visualise single molecules and this can lead to rapid photobleaching of FPs. When immobilised, a single FP can be observed until it is irreversibly photobleached, which occurs after 1 to 10 seconds in typical microscope-based experiments. In solution, single molecules can be detected as they pass through a focused laser beam, a process which typically takes less than a millisecond. Fluctuations in intensity therefore primarily measure the translational diffusion properties of the FP (or its attached fusion protein). However, if there are any fluctuations in intensity due to chemical reactions (*e.g.* protonation) during this time period, they will be superimposed on the diffusional fluctuations and can be resolved by autocorrelation analysis. This is the basis of fluorescence correlation spectroscopy (FCS). Thus, dynamic processes in the μs range can be studied using FCS. FCS can operate at the single molecule level, but the signal is built up from many different single molecules, and hence reports on the population as a whole.

Blinking in FPs. When FPs are observed at the single molecule level they often "blink". 'Blinking' (that is, the fluctuation of emission levels—between 'light' and 'dark' states—despite continuous excitation) can occur on many timescales from μs to s. Rapid blinking may arise because the excited singlet state is converted to a longer-lived triplet state. eYFP blinks on the seconds timescale in saline buffers

due to the slow proton-coupled chloride-binding reaction that is readily seen in ensemble stopped-flow measurements (see Fig. 5). A time course of a typical blinking time trace is shown in Fig. 10.[23]

This form of blinking is independent of the excitation process and may complicate the interpretation of some kinetic experiments. For example, if the binding of an FP-tagged protein to another protein is studied by single molecule fluorescence microscopy, it may be difficult to determine whether the disappearance and reappearance of a fluorescent spot is due to dissociation and reassociation of the proteins of interest or to FP blinking. Blinking may also be driven by the excitation process itself. Indeed, reversible photobleaching (see above) can give rise to blinking if the excitation wavelength employed is absorbed by both the light and dark states. We have observed that the laser light intensities required to visualise single molecules can drive the protonation reaction of eYFP and increases the blinking rate, which ultimately leads to irreversible photobleaching.

FCS studies on GFP Ser65Thr and eGFP observed dynamics from only one dark state at pH $>$ 8 (excitation at 488 nm). At pH $<$ 7, additional relaxation processes were present (which are probably due to protonation from the bulk solvent).[46] However, results for eGFP have also been shown to be dependent on the ionic strength of the buffer. Studies on the related mutant GFPmut2 (Ser65Ala, Val68Leu, Ser72Ala) using two-colour excitation FCS spectroscopy[47] also suggest that there are two pH mediated relaxation modes. At low external pH, a faster process (10–100 μs) dominates. A slower form of excitation-dependent process in the 100–500 μs range is observed at higher pH and assigned to a structural change. For the YFP class of mutants, the observations are much more buffer dependent. As mentioned above, single molecule studies in chloride buffer observed blinking on the seconds timescale. Other studies on these YFP mutants in saline-free phosphate buffer did not observe an external pH dependence in the excitation-driven dynamics and concluded that the excitation-driven dark state was distinct from the protonated dark state on the FCS timescale.[48] As remarked in that study, FCS observes processes in the microsecond range and therefore does not observe slower processes in the millisecond and especially on the seconds timescale that have been observed for this class of avGFP mutants in the absence of salt in bulk kinetic studies.

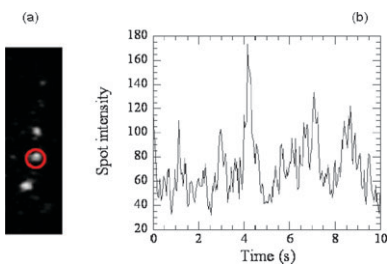

Fig. 10 (a) Single frame capture of single YFP–myosin II head (*Dictyostelium*) molecules attached to an actin filament. (b) Time course of fluorescence emission of a single molecule (circled in red in (a)) showing blinking on the seconds timescale. Buffers were 40 mM NaCl, 2 mM $MgCl_2$, 0.1 mM EGTA, 10 mM dithiothreitol, 20 mM Hepes at pH 7.5 and 20 °C.

Fluorescence decay data of native and irradiated protein indicate that dark states are present in red-emitting FPs, such as eqFP611 Val124Thr.[39] In the DsRed variants, mRFP, mCherry and mStrawberry, dark states are found to be light induced. These dark states are observed to exist more often and longer with increasing pH.[49] Again, at pH values $<$5, additional fast processes are observed and are likely to be due to protonation of the chromophore by the bulk solvent.

Photoactivated localisation microscopy (PALM)

In conventional fluorescence microscopy, particles can be resolved if they are separated by more than about 200 nm (the diffraction limit of 400 nm light). Single molecules, however, can be localised to 1 nm if they emit enough photons and there are no similarly emitting molecules within ~200 nm, by estimating the centre of the 2D Gaussian profile of the spot. Some forms of super-resolution microscopy (*e.g.* PALM) effectively build up an image from individual single molecule localisations with nanometre precision.[50] In densely labelled samples, individual fluorophores are localised by sequentially switching them on and off with light of different wavelengths. In practice, resolution was improved to ~50–100 nm resolution in all directions, when used in combination with TIRF. Axial resolution has now been improved to sub-20 nm with the use of interferometric PALM (iPALM),[51] in which the emitted photon from the photon source (the FP) is used as its own reference, travels through two distinct optical paths and is recombined so as to interfere with itself. The axial position of the photon source is determined by the relative amplitude of the output beams.

The ideal FP for PALM would be monomeric, bright (high molecular extinction coefficient and quantum yield) with high contrast (low background noise) and its switching properties (dark/bright or wavelength shift) should be well-controlled by the activating light with little spontaneous interconversion between the states. In addition, the rate of activation/deactivation must be balanced so that only a few molecules are in the fluorescent state at any given time. This perfect FP does not yet exist, but there are many new variants currently being produced and characterised, and recent examples include IrisFP[42] and mEos2.[52] The major advantage of FPs in super-resolution imaging is that they can be targeted to specific proteins, but non-proteinaceous fluorophores still tend to be smaller, brighter and more controllable.

Examples of photoconvertible FPs. Three classes of FPs have been used for super-resolution imaging: photoactivable (kindling), photoshiftable and reversibly photoactivable FPs. A mutant of avGFP, commonly called photoactivatable GFP or PA-GFP (Phe99Ser, Met153Thr, Val163Ala, Thr203His), has a neutral chromophore in its native state but undergoes an irreversible photoactivation on irradiation at 405 nm to produce an anionic form *via* the decarboxylation of Glu222.[53] Dronpa is a reversibly photoactivable FP. IrisFP is an example of both a photoactivable (green-dark, red-dark) and a photoshiftable (green to red) FP and has been described previously.

Fluorescence recovery after photobleaching (FRAP)

This technique is used to study the localisation and kinetic behaviour of FP-tagged proteins.[54,55] Intense illumination

locally bleaches the fluorophore and diffusion or fresh synthesis of the FP-tagged protein restores fluorescence in this area and is recorded using low level excitation microscopy. Quantitative studies can provide an estimation of the effective diffusion coefficient (D_{eff}) and mobile fraction (M_f) of a protein. If the FP-tagged protein interacts with another component that is static, then the recovery profile will reflect both the association and dissociation kinetics, as well as the diffusion of the FP-tagged protein (Fig. 11). In some cases, one of these contributions may dominate. The hallmark of a significant contribution from diffusion is that the recovery profile shows a dependence on the area that is bleached. In the context of this review, an important control is to demonstrate that recovery of FP-fluorescence is not due to reversible photobleaching of the FP itself. This can be done using fixed cells, in which the FP-tagged protein is unable to diffuse and therefore they should show no recovery following bleaching.

In fluorescence imaging experiments, eCFP has been observed to show reversible photobleaching under laser excitation at 458 nm, which recovers spontaneously in the dark almost to initial levels.[56] Illumination at 430 nm also induced recovery of fluorescence. eYFP also shows some spontaneous recovery following photobleaching at 514 nm.[23]

Protein diffusion and trafficking when fused to FPs within live cells can be monitored by the several techniques, for example, single particle tracking (which may be complicated by blinking events), fluorescence correlation spectroscopy and the photoconversion methods, in which proteins are highlighted or their emissions shifted by laser illumination. These local populations of protein can be visualised and then followed as they diffuse or travel within the cell. 'Timer' FPs such as the E5 mutant of DsRed[57] can also be useful in studies of protein synthesis and turnover; these initially produce a green-emitting fluorophore which converts to red-emitting over time. The conversion process appears to be concentration independent. The age of a protein tagged with a 'Timer' FP can be determined by the green to red fluorescence ratio.

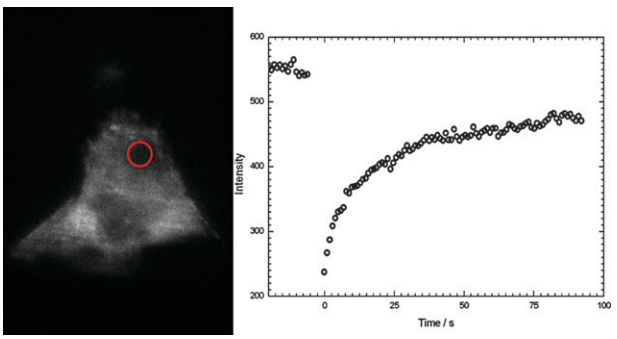

Fig. 11 TIRF image of an A431/SIP1 cell expressing GFP–myosin heavy chain IIA and FRAP trace. The graph shows the fluorescence intensity of the area circled in red which was bleached for 2 seconds with an intense confocal 488 nm beam. This cell is also expressing S100A4 which has the potential to solubilise myosin filaments and may account for the relatively rapid recovery in fluorescence because of the high concentration of monomeric GFP–myosin. (In collaboration with Drs S. K. Badyal and M. Kriajevska).

Förster (fluorescence) resonance energy transfer (FRET)

FRET is widely used to determine the proximity between two proteins (or more exactly the fluorescence probes attached to the proteins) or to monitor movement between domains within a protein.[58,59] It is also the basis of many sensors in which a small ligand (*e.g.* Ca^{2+}) binding to a protein domain is monitored by a pair of FPs attached to the N and C termini. For many cell biological applications, accurate measurement of energy transfer is more important than the uncertainties in the application of the Förster equation to determine distance between the fluorophores because only a binary answer is required to test for protein interaction (*i.e.* FRET or no FRET). However, there are still pitfalls in measuring FRET efficiency using FPs. Firstly, the concentration of the two FPs must be comparable, otherwise the bleed-through (cross-talk) from one FP into the detector channel of the other will swamp any changes due to FRET. This is not a problem when the two FPs are fused to the same protein, although even here their concentration may not be identical due to different folding efficiencies. A guide to selection of suitable FPs for FRET pairs can be found in ref. 11, 45 and chapter 5 of ref. 47.

FRET efficiency is determined not only by the distance (r) between the donor and acceptor (<10 nm with a sixth power dependence) but also by the Förster distance (R_0) that incorporates contributions from the spectral overlap of the donor emission and acceptor absorbance, their quantum yield and extinction coefficients, respectively, and the orientation of their dipole moments (κ^2). FRET efficiency is measured experimentally using donor intensity quenching, donor lifetime shortening, or acceptor fluorescence sensitisation. In the first two methods, donor intensity and lifetime changes are determined in the absence of an acceptor as a reference point.

Photobleached FRET artifacts. Acceptor photobleaching is commonly used to quantify FRET (*e.g.* in CFP–YFP FRET pairs), where the increase in donor CFP emission intensity is measured on the loss of YFP acceptor absorbance. Nevertheless, what is monitored under the microscope is loss of acceptor fluorescence following photobleaching. It is usually assumed that the absorbance is lost as well, but rarely is this checked explicitly. Fortunately for YFP, bleaching results in proportional loss of 514 nm absorbance but new absorption peaks appear in the 390–420 nm region, overlapping with the donor CFP (for an example of a photobleached YFP absorbance spectrum see Fig. 12).[23]

To complicate matters, the bleached YFP, when excited at 420 nm, shows weak emission in the 460 nm region[23] that potentially can contribute to the CFP channel and hence can lead to an overestimate of the dequenching of the donor.[60,61] Furthermore, when the CFP channel is examined after photobleaching of the YFP acceptor, the excitation light used (380 nm) can activate the bleached YFP to regenerate the fluorescent YFP anion, which will lead to an underestimate of donor dequenching.[23,62]

The problem of the orientation factor, κ^2, with respect to FPs. For quantitative interpretation of FRET further complications must be considered. With regard to the Förster equation, the uncertainty in the orientation factor has received much

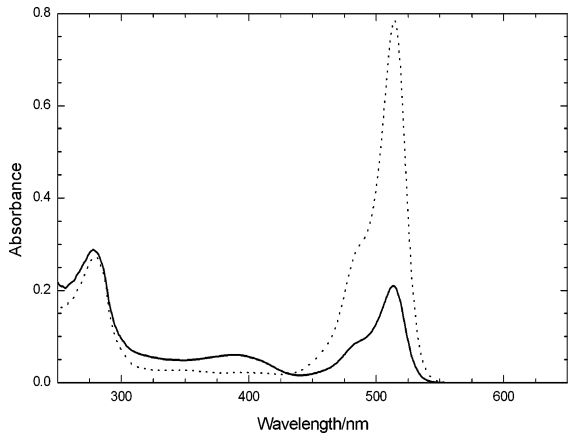

Fig. 12 74% photobleached YFP (solid line). Peak at 395 nm is due to the irreversibly bleached form. Starting material shown as dotted line.

discussion over the years.[63,64] The value of 2/3 is derived for the case of rapidly tumbling fluorophores whose motion is fast relative to their fluorescence lifetime. This does not apply to fluorescent proteins, whose anisotropy values of $\sim$0.3 indicate that they tumble slowly. If for some reason the proteins are held rigidly with respect to each other (*e.g.* due to short linkers or intramolecular association between domains), there remains considerable uncertainty in the value of κ^2. In the case of a myosin motor domain fusion construct, the contour plots of ref. 63 indicated a possible range of κ^2 from about 0.1 to 3 with the most probable value at the low end.[22] However, if the FRET pairs can take range of orientations with respect to each other (*i.e.* static disorder), the uncertainty in R_0 introduced by assuming $\kappa^2 = 2/3$ is likely to be $<$25% and less than the uncertainty in κ^2 because of the 6th power dependence of R_0, as well as the bias in energy transfer towards higher κ^2 values.[64] Nevertheless, this does not justify the common procedure of assuming $\kappa^2 = 2/3$ unless a large static disorder of the FRET probes is proven.

Inter and intramolecular dimerisation of FPs within FRET pairs. The tendency of FPs to dimerise can, in itself, perturb measurements of association between FP-tagged proteins and is best minimised by using monomer variants (*e.g.* Ala206Lys). Association between FPs can also perturb their absorption and fluorescence properties and give rise to artifacts in FRET.[22] For example, a fusion probe for FRET studies, BFP–myosin–GFP, was shown to have an apparent 40% reduction in acceptor fluorescence on binding its substrate, ATP. A similar construct, CFP–myosin–YFP showed only minor changes on ATP binding ($\sim$5%). As mentioned before, dimerisation of GFP with the BFP drives the GFP absorption spectrum towards the protonated form and excitation at 380 nm (to excite the BFP donor) actually gives emission at 510 nm *via* ESPT from GFPH, which gives the appearance of FRET. The true FRET result of substrate binding is seen with the CFP–myosin–YFP construct. While the original BFP–GFP pair is no longer used due to the poor photostability of BFP, eGFP remains in use in techniques such as bioluminescence resonance energy transfer (BRET), and is now often used in conjunction with red FPs such as mCherry as a FRET pair. Where interprobe dimerisation is a possibility, the Ala206Lys mutation should be incorporated into eGFP. However, changes in protonation state in themselves can be exploited to monitor interactions. Proximity imaging (PRIM) uses the changes in relative intensity of the absorption bands or fluorescence excitation spectra of GFP on dimerisation to quantitatively image the homo-oligomerisation or clustering processes of GFP-tagged proteins *in vivo*.[65,66]

Conclusions

Understanding the photophysics and photochemistry of FPs is key to their use in a variety of techniques as biological probes. While wild-type avGFP continues to present physical chemists with a challenging system to be probed with increasing time and spatial resolution, molecular biologists have prepared a dazzling array of new proteins using a combination of rational design and screening of random mutants. In many of these new variants, a trait in the wild-type protein is suppressed or enhanced to give a desired property and therefore the detailed study of these new constructs can help understand the basic photochemical properties of the parent construct. In this review we have highlighted the complexities of FPs which initially may have complicated their characterisation, but subsequently have been exploited to probe biological systems in greater detail.

Acknowledgements

We thank Dr Xinghua Shi and Dr Jasper Van Thor for helpful suggestions and contributions. HES and CRB are supported by the Leverhulme Trust.

Notes and references

1 O. Shimomura, *J. Microsc.*, 2005, **217**, 1–15.
2 O. Shimomura, *FEBS Lett.*, 1979, **104**, 220–222.
3 R. Y. Tsien, *Annu. Rev. Biochem.*, 1998, **67**, 509–544.
4 R. M. Wachter, *Acc. Chem. Res.*, 2007, **40**, 120–127.
5 W. W. Ward, H. J. Prentice, A. F. Roth, C. W. Cody and S. C. Reeves, *Photochem. Photobiol.*, 1982, **35**, 803–808.
6 J. J. van Thor, T. Gensch, K. J. Hellingwerf and L. N. Johnson, *Nat. Struct. Biol.*, 2002, **9**, 37–41.
7 M. B. Elowitz, M. G. Surette, P. E. Wolf, J. Stock and S. Leibler, *Curr. Biol.*, 1997, **7**, 809–812.
8 M. Chattoraj, B. A. King, G. U. Bublitz and S. G. Boxer, *Proc. Natl. Acad. Sci. U. S. A.*, 1996, **93**, 8362–8367.
9 N. Agmon, *J. Phys. Chem. A*, 2005, **109**, 13–35.
10 W. L. DeLano, The PyMOL Molecular Graphics System, http://www.pymol.org.
11 N. Agmon, *Biophys. J.*, 2005, **88**, 2452–2461.
12 D. Stoner-Ma, A. A. Jaye, P. Matousek, M. Towrie, S. R. Meech and P. J. Tonge, *J. Am. Chem. Soc.*, 2005, **127**, 2864–2865.
13 J. J. van Thor, G. Zanetti, K. L. Ronayne and M. Towrie, *J. Phys. Chem. B*, 2005, **109**, 16099–16108.
14 P. Leiderman, D. Huppert and N. Agmon, *Biophys. J.*, 2006, **90**, 1009–1018.
15 N. C. Shaner, P. A. Steinbach and R. Y. Tsien, *Nat. Methods*, 2005, **2**, 905–909.
16 R. M. Wachter and S. J. Remington, *Curr. Biol.*, 1999, **9**, R628–629.
17 D. Arosio, G. Garau, F. Ricci, L. Marchetti, R. Bizzarri, R. Nifosi and F. Beltram, *Biophys. J.*, 2007, **93**, 232–244.
18 R. M. Wachter, D. Yarbrough, K. Kallio and S. J. Remington, *J. Mol. Biol.*, 2000, **301**, 157–171.
19 O. Griesbeck, G. S. Baird, R. E. Campbell, D. A. Zacharias and R. Y. Tsien, *J. Biol. Chem.*, 2001, **276**, 29188–29194.

20 X. Shi, J. Basran, H. E. Seward, W. Childs, C. R. Bagshaw and S. G. Boxer, *Biochemistry*, 2007, **46**, 14403–14417.
21 R. Bizzarri, R. Nifosi, S. Abbruzzetti, W. Rocchia, S. Guidi, D. Arosio, G. Garau, B. Campanini, E. Grandi, F. Ricci, C. Viappiani and F. Beltram, *Biochemistry*, 2007, **46**, 5494–5504.
22 W. Zeng, H. E. Seward, A. Malnasi-Csizmadia, S. Wakelin, R. J. Woolley, G. S. Cheema, J. Basran, T. R. Patel, A. J. Rowe and C. R. Bagshaw, *Biochemistry*, 2006, **45**, 10482–10491.
23 T. B. McAnaney, W. Zeng, C. F. Doe, N. Bhanji, S. Wakelin, D. S. Pearson, P. Abbyad, X. Shi, S. G. Boxer and C. R. Bagshaw, *Biochemistry*, 2005, **44**, 5510–5524.
24 D. A. Zacharias, J. D. Violin, A. C. Newton and R. Y. Tsien, *Science*, 2002, **296**, 913–916.
25 M. H. Seifert, J. Georgescu, D. Ksiazek, P. Smialowski, T. Rehm, B. Steipe and T. A. Holak, *Biochemistry*, 2003, **42**, 2500–2512.
26 S.-T. D. Hsu, C. Behrens, L. D. Cabrita and C. M. Dobson, *Biomol. NMR Assign.*, 2009, **3**, 67–72.
27 M. V. Matz, A. F. Fradkov, Y. A. Labas, A. P. Savitsky, A. G. Zaraisky, M. L. Markelov and S. A. Lukyanov, *Nat. Biotechnol.*, 1999, **17**, 969–973.
28 A. S. Mishin, F. V. Subach, I. V. Yampolsky, W. King, K. A. Lukyanov and V. V. Verkhusha, *Biochemistry*, 2008, **47**, 4666–4673.
29 N. C. Shaner, R. E. Campbell, P. A. Steinbach, B. N. Giepmans, A. E. Palmer and R. Y. Tsien, *Nat. Biotechnol.*, 2004, **22**, 1567–1572.
30 L. Wang, W. C. Jackson, P. A. Steinbach and R. Y. Tsien, *Proc. Natl. Acad. Sci. U. S. A.*, 2004, **101**, 16745–16749.
31 X. Shu, L. Wang, L. Colip, K. Kallio and S. J. Remington, *Protein Sci.*, 2009, **18**, 460–466.
32 P. Abbyad, W. Childs, X. Shi and S. G. Boxer, *Proc. Natl. Acad. Sci. U. S. A.*, 2007, **104**, 20189–20194.
33 X. Shu, N. C. Shaner, C. A. Yarbrough, R. Y. Tsien and S. J. Remington, *Biochemistry*, 2006, **45**, 9639–9647.
34 R. Ando, H. Mizuno and A. Miyawaki, *Science*, 2004, **306**, 1370–1373.
35 S. Habuchi, R. Ando, P. Dedecker, W. Verheijen, H. Mizuno, A. Miyawaki and J. Hofkens, *Proc. Natl. Acad. Sci. U. S. A.*, 2005, **102**, 9511–9516.
36 R. Nifosi, A. Ferrari, C. Arcangeli, V. Tozzini, V. Pellegrini and F. Beltram, *J. Phys. Chem. B*, 2003, **107**, 1679–1684.
37 J. Petersen, P. G. Wilmann, T. Beddoe, A. J. Oakley, R. J. Devenish, M. Prescott and J. Rossjohn, *J. Biol. Chem.*, 2003, **278**, 44626–44631.
38 H. W. Ai, J. N. Henderson, S. J. Remington and R. E. Campbell, *Biochem. J.*, 2006, **400**, 531–540.
39 D. C. Loos, S. Habuchi, C. Flors, J. Hotta, J. Wiedenmann, G. U. Nienhaus and J. Hofkens, *J. Am. Chem. Soc.*, 2006, **128**, 6270–6271.
40 M. Andresen, M. C. Wahl, A. C. Stiel, F. Grater, L. V. Schafer, S. Trowitzsch, G. Weber, C. Eggeling, H. Grubmuller, S. W. Hell and S. Jakobs, *Proc. Natl. Acad. Sci. U. S. A.*, 2005, **102**, 13070–13074.
41 H. Mizuno, T. K. Mal, M. Walchli, A. Kikuchi, T. Fukano, R. Ando, J. Jeyakanthan, J. Taka, Y. Shiro, M. Ikura and A. Miyawaki, *Proc. Natl. Acad. Sci. U. S. A.*, 2008, **105**, 9227–9232.
42 V. Adam, M. Lelimousin, S. Boehme, G. Desfonds, K. Nienhaus, M. J. Field, J. Wiedenmann, S. McSweeney, G. U. Nienhaus and D. Bourgeois, *Proc. Natl. Acad. Sci. U. S. A.*, 2008, **105**, 18343–18348.
43 G. J. Kremers, K. L. Hazelwood, C. S. Murphy, M. W. Davidson and D. W. Piston, *Nat. Methods*, 2009, **6**, 355–358.
44 M. Chalfie, Y. Tu, G. Euskirchen, W. Ward and D. Prasher, *Science*, 1994, **263**, 802–805.
45 M. Chalfie and S. R. Kain, *Green Fluorescent Protein: Properties, Applications and Protocols*, Wiley Interscience, Hoboken, New Jersey, 2006.
46 U. Haupts, S. Maiti, P. Schwille and W. W. Webb, *Proc. Natl. Acad. Sci. U. S. A.*, 1998, **95**, 13573–13578.
47 C. Bosisio, V. Quercioli, M. Collini, L. D'Alfonso, G. Baldini, S. Bettati, B. Campanini, S. Raboni and G. Chirico, *J. Phys. Chem. B*, 2008, **112**, 8806–8814.
48 P. Schwille, S. Kummer, A. A. Heikal, W. E. Moerner and W. W. Webb, *Proc. Natl. Acad. Sci. U. S. A.*, 2000, **97**, 151–156.
49 J. Hendrix, C. Flors, P. Dedecker, J. Hofkens and Y. Engelborghs, *Biophys. J.*, 2008, **94**, 4103–4113.
50 M. Fernández-Suárez and A. Ting, *Nat. Rev. Mol. Cell Biol.*, 2008, **9**, 929–943.
51 G. Shtengel, J. A. Galbraith, C. G. Galbraith, J. Lippincott-Schwartz, J. M. Gillette, S. Manley, R. Sougrat, C. M. Waterman, P. Kanchanawong, M. W. Davidson, R. D. Fetter and H. F. Hess, *Proc. Natl. Acad. Sci. U. S. A.*, 2009, **106**, 3125–3130.
52 S. A. McKinney, C. S. Murphy, K. L. Hazelwood, M. W. Davidson and L. L. Looger, *Nat. Methods*, 2009, **6**, 131–133.
53 J. N. Henderson, R. Gepshtein, J. R. Heenan, K. Kallio, D. Huppert and S. J. Remington, *J. Am. Chem. Soc.*, 2009, **131**, 4176–4177.
54 B. L. Sprague and J. G. McNally, *Trends Cell Biol.*, 2005, **15**, 84–91.
55 J. Lippincott-Schwartz and G. H. Patterson, *Science*, 2003, **300**, 87–91.
56 D. Sinnecker, P. Voigt, N. Hellwig and M. Schaefer, *Biochemistry*, 2005, **44**, 7085–7094.
57 A. Terskikh, A. Fradkov, G. Ermakova, A. Zaraisky, P. Tan, A. V. Kajava, X. Zhao, S. Lukyanov, M. Matz, S. Kim, I. Weissman and P. Siebert, *Science*, 2000, **290**, 1585–1588.
58 T. W. J. Gadella, *FRET and FLIM techniques*, Elsevier, Amsterdam, 2009.
59 A. Muller-Taubenberger and K. I. Anderson, *Appl. Microbiol. Biotechnol.*, 2007, **77**, 1–12.
60 G. Valentin, C. Verheggen, T. Piolot, H. Neel, M. Coppey-Moisan and E. Bertrand, *Nat. Methods*, 2005, **2**, 801.
61 M. T. Kirber, K. Chen and J. F. Keaney, Jr., *Nat. Methods*, 2007, **4**, 767–768.
62 A. Miyawaki and R. Y. Tsien, *Methods Enzymol.*, 2000, **327**, 472–500.
63 R. E. Dale, J. Eisinger and W. E. Blumberg, *Biophys. J.*, 1979, **26**, 161–193.
64 B. W. van der Meer, *Rev. Mol. Biotechnol.*, 2002, **82**, 181–196.
65 D. A. De Angelis, G. Miesenbock, B. V. Zemelman and J. E. Rothman, *Proc. Natl. Acad. Sci. U. S. A.*, 1998, **95**, 12312–12316.
66 S. Iwai and T. Q. Uyeda, *Proc. Natl. Acad. Sci. U. S. A.*, 2008, **105**, 16882–16887.